



## Technical Note: Modulation of fMRI brainstem responses by transcutaneous vagus nerve stimulation

Diba Borgmann<sup>a,b,c,\*</sup>, Lionel Rigoux<sup>b,d</sup>, Bojana Kuzmanovic<sup>b</sup>, Sharmili Edwin Thanarajah<sup>b,e</sup>, Thomas F. Münte<sup>g</sup>, Henning Fenselau<sup>a,f,h</sup>, Marc Tittgemeyer<sup>b,f</sup>

<sup>a</sup> Synaptic Transmission in Energy Homeostasis Group, Max Planck Institute for Metabolism Research, Gleueler Strasse 50, 50931, Cologne, Germany

<sup>b</sup> Translational Neurocircuitry Group, Max Planck Institute for Metabolism Research, Gleueler Strasse 50, 50931, Cologne, Germany

<sup>c</sup> Center for Anatomy II, Neuroanatomy, University Hospital Cologne, Joseph-Stelzmann Str. 9, 50937, Cologne, Germany

<sup>d</sup> Translational Neuromodeling Unit, Institute for Biomedical Engineering, Swiss Federal Institute of Technology, Wilfriedstrasse 6, 8032, Zurich, Switzerland

<sup>e</sup> Department of Psychiatry, Psychosomatics and Psychotherapy, University Hospital Frankfurt, 60528, Frankfurt, Germany

<sup>f</sup> Cluster of Excellence in Cellular Stress Responses in Aging Associated Diseases (CECAD), University of Cologne, 50931, Cologne, Germany

<sup>g</sup> Department of Neurology, University of Lübeck, 23538, Lübeck, Germany

<sup>h</sup> Center for Endocrinology, Diabetes and Preventive Medicine (CEDP), University Hospital Cologne, Kerpener Strasse 26, 50924, Cologne, Germany

### A B S T R A C T

Our increasing knowledge about gut-brain interaction is revolutionising the understanding of the links between digestion, mood, health, and even decision making in our everyday lives. In support of this interaction, the vagus nerve is a crucial pathway transmitting diverse gut-derived signals to the brain to monitor of metabolic status, digestive processes, or immune control to adapt behavioural and autonomic responses. Hence, neuromodulation methods targeting the vagus nerve are currently explored as a treatment option in a number of clinical disorders, including diabetes, chronic pain, and depression. The non-invasive variant of vagus nerve stimulation (VNS), transcutaneous auricular VNS (taVNS), has been implicated in both acute and long-lasting effects by modulating afferent vagus nerve target areas in the brain. The physiology of neither of those effects is, however, well understood, and evidence for neuronal response upon taVNS in vagal afferent projection regions in the brainstem and its downstream targets remain to be established.

Therefore, to examine time-dependent effects of taVNS on brainstem neuronal responses in healthy human subjects, we applied taVNS during task-free fMRI in a single-blinded crossover design. During fMRI data acquisition, we either stimulated the left earlobe (sham), or the target zone of the auricular branch of the vagus nerve in the outer ear (cymba conchae, verum) for several minutes, both followed by a short 'stimulation OFF' period. Time-dependent effects were assessed by averaging the BOLD response for consecutive 1-minute periods in an ROI-based analysis of the brainstem.

We found a significant response to acute taVNS stimulation, relative to the control condition, in downstream targets of vagal afferents, including the nucleus of the solitary tract, the substantia nigra, and the subthalamic nucleus. Most of these brainstem regions remarkably showed increased activity in response to taVNS, and these effect sustained during the post-stimulation period. These data demonstrate that taVNS activates key brainstem regions, and highlight the potential of this approach to modulate vagal afferent signalling. Furthermore, we show that carry-over effects need to be considered when interpreting fMRI data in the context of general vagal neurophysiology and its modulation by taVNS.

### 1. Introduction

The central nervous system (CNS) constantly monitors bodily signals and adapts behavioural and physiological responses to maintain physiological homeostasis. To regulate energy and glucose metabolism and to adapt feeding behaviour, for instance, the CNS exerts efferent control on gastric tone and emptying, or levels of gut-derived humoral or neural signals (Clemmensen et al., 2017). For this to be possible, the brain relies on the reception of a vast array of peripheral signals from different organs (Egerod et al., 2019; Fülling et al., 2019; Kim et al., 2018; Yu et al., 2020). In this context, the vagus nerve has recently gained specific attention, as a crucial bi-directional pathway in communicating signals between body and brain (Alhadeff, 2021; Cork, 2018; Travagli and Anselmi, 2016).

The afferent vagus comprises distinct fibre types innervating wide parts of thoracic and abdominal organs, including the gut, heart and lung, as well as parts of the pinna and meninges (Butt et al., 2020). Vagal afferent information converges in the nucleus of the solitary tract (NTS), a bilateral V-shaped nucleus spanning the caudal medulla at the level of the obex. While the nucleus itself is thought to be compartmentalized regarding the origin of afferents, as reported in anatomical and clinical studies (Barraco, 1994; Cutsforth-Gregory and Benarroch, 2017), recent work points towards heterogenous cell populations, some of which are activated along the entire nucleus in response to peripheral signals (Chen et al., 2020; Han et al., 2018; Tan et al., 2020). This supports the concept of intranuclear connectivity rather than strict topographical organization alone, which in turn could allow for multi-sensory integration of signals from different organs and their transmission into specific downstream circuits. Thus, the NTS seems to be op-

\* Corresponding author at: Max Planck Institute for Metabolism Research, Gleueler Str. 50, 50931 Cologne, Germany.

E-mail address: [diba.borgmann@sf.mpg.de](mailto:diba.borgmann@sf.mpg.de) (D. Borgmann).

<https://doi.org/10.1016/j.neuroimage.2021.118566>.

Received 1 April 2021; Received in revised form 20 July 2021; Accepted 7 September 2021

Available online 10 September 2021.

1053-8119/© 2021 The Authors. Published by Elsevier Inc. This is an open access article under the CC BY-NC-ND license (<http://creativecommons.org/licenses/by-nc-nd/4.0/>)

timally composed to serve as the main hub to convey afferent vagal signals into different neurocircuits, for instance to provide input to the parabrachial area (e.g. Borgmann et al., 2021), hypothalamic regions (e.g. Goldstein et al., 2021) and the bed nucleus of the stria terminalis (BNST; Ch'ng et al., 2018; Lebow and Chen, 2016; Stamatakis et al., 2014). Consistent with this, mouse models have shown that stimulating gut-innervating vagal afferents drives preference learning through the activation of dopamine-dependent nigro-striatal pathways via the NTS (Han et al., 2018). Furthermore, vagal afferents include fibres that sense mechanical stimuli, such as intestinal stretch, which reduce food intake upon artificial stimulation (Bai et al., 2019), and some that sense sugar in the gut and drive preference learning via downstream activation of NTS neurons (Tan et al., 2020). Together, these findings support the concept of a body-vagal-brain axis mediating diverse homeostatic regulation processes, with vagal afferents sensing interoceptive signals from the body and conveying them to the brain via the NTS.

Given the importance of vagal afferents in informing the brain of bodily states, methods enabling a selective manipulation of its function represent a promising approach, not least for basic sciences to enhance our understanding of body-brain communication. Beyond, neuromodulation approaches targeting the vagus nerve have been explored as potential treatment options for various clinical disorders, including diabetes, heart failure, bowel disease, depression, epilepsy, and headache syndromes (de Lartigue, 2016; Kaniusas et al., 2019b). Transcutaneous auricular vagus nerve stimulation (taVNS), applied non-invasively to the exclusively afferent auricular branch of the vagus nerve (Butt et al., 2020), might allow for such a selective modulation of vagus-downstream neurocircuitry (Alicart et al., 2020; Koenig et al., 2021; Kuhnel et al., 2020; Liu et al., 2020; Neuser et al., 2020; Obst et al., 2020; von Wrede et al., 2021). It remains, however, unclear how taVNS modulates individual brain regions that control behavioural responses.

Previous studies demonstrated that VNS, applied either transcutaneously or via an implanted stimulator, regulates downstream targets of vagal afferents through different neurotransmitter systems (e.g., Colzato and Beste, 2020; Hachem et al., 2018). Its success in anticonvulsive therapy, for example, is thought to be mediated by the modulation of gamma-aminobutyric acid (GABA) release, as determined through behavioural and electrophysiological measures of automated motor inhibition after taVNS (Keute et al., 2018), or directly through elevated cerebrospinal fluid (CSF)-GABA levels in response to invasive stimulation of the cervical vagus nerve in patients with partial seizures (Ben-Menachem et al., 1995). In addition, the locus coeruleus (LC) – a major norepinephrine brainstem nucleus that receives vagal input via the nucleus of the solitary tract (Aston-Jones et al., 2004) – has been shown to be modulated by taVNS in various human neuroimaging studies (Frangos et al., 2015; Kraus et al., 2013; Yakunina et al., 2017), although pupillometry as an indirect measure of norepinephrine (NE) release from the LC failed to show significant differences between sham and verum taVNS (Keute et al., 2019; Warren et al., 2019). Furthermore, reciprocal connections between the dorsal raphe nuclei (DRN) and the LC enable cross-modulatory regulation of adrenergic and serotonergic transmitter release (Brown et al., 2002). Accordingly, anti-depressive effects of (ta)VNS are hypothesized to be, at least partially, based on the modulation of serotonin levels, in close interactions with NE release. Extended invasive VNS potently increases the firing rates of the DRN and LC, as shown by extracellular recordings in the rat throughout a long-term (90-day) stimulation protocol (Dorr and Debonnel, 2006), indicating effects via the induction of neuroplasticity. Consistent with this finding in rats, taVNS elicited changes in the functional connectivity between midline cortical structures and the orbitofrontal cortex, among others, along with the alleviation of symptoms in patients suffering from Major Depression (Fang et al., 2016).

In the present study, we aimed to evaluate the modulatory potential of taVNS on brainstem activity in a single-blind, crossover functional magnetic resonance (fMRI) study. Given that both acute and long-lasting effects of taVNS might exist (Szeska et al., 2020), we did not apply a

classical task-related fMRI design, as the neural responses to alternating periods of sham and verum stimulation would be challenging to interpret due to possible carry-over effects. Instead, we conducted a task-free measurement with three different blocks: baseline (stimulation OFF), sham or verum stimulation, and post-stimulation (stimulation OFF). In order to assess the temporal dynamics of taVNS' effects on brainstem activity, we analysed BOLD signals averaged across 1-minute time bins, each contrasted with the baseline, and focused on both acute effects during the stimulation and on prolonged effects following the stimulation. Hence, by following the argumentation that stimulation of the auricular branch of the vagus nerve increases input to the NTS in the medulla and influences the activity of NTS neurons, we hypothesized that brainstem areas known to be targeted by vagal afferents in mice would also be activated by taVNS in an acute and prolonged manner.

## 2. Methods and materials

### 2.1. Participants

Fifteen lean, healthy probands were recruited from a database maintained at the Max-Planck Institute for Metabolism Research, Cologne. All participants were non-smokers, without a history of neurological, psychiatric, gastrointestinal, cardiac or eating disorders, and without any special diets or medical treatments. Three subjects were excluded due to excessive motion during fMRI measurement. In total, 12 subjects (8 females, aged  $29.1 \pm 1.3$  years, BMI  $22.5 \pm 0.7$ ) were included in further data analyses.

All participants gave written informed consent to participate in the experiment, which was approved by the local ethics committee of the Medical Faculty of the University of Cologne (Cologne, Germany; No: 16-229).

### 2.2. Experimental design

The study was carried out in a single-blinded, sham-controlled, crossover design (Fig. 1). Each volunteer participated in two subsequent runs within the same fMRI session. To avoid potential carry-over effects, each participant first received the sham stimulation before entering the session with verum stimulation.

On the testing day, prior to subjects' placement in the scanner, individuals were introduced to the experimental procedure. Irrespective of the session (sham or verum), participants' individual sensory and pain thresholds were defined before functional image acquisition for both stimulation sites –left earlobe for sham and left cymba conchae for verum stimulation, respectively, using a transcutaneous nerve stimulator (NEMOS, Cerbomed, Erlangen, Germany). Starting with 0.1mA (cf. Frangos et al., 2015) and increasing in 0.1mA steps, the emergence of a tingling sensation was set as the lower sensory stimulation threshold. The beginning of a painful sensation or an intolerable sensation of discomfort determined the upper stimulation threshold. Final stimulation intensity was set to 0.1 mA beneath the upper threshold without going over 0.5mA. Average recorded final stimulation intensity ( $\pm$  SD) was  $0.41 \pm 0.13$ mA (range 0.1 - 0.5mA) for earlobe stimulation, and  $0.31 \pm 0.19$ mA (range 0.1 - 0.5mA) for stimulation of the cymba conchae. Stimulation was applied in 0.25ms duration monophasic square wave pulses at 25Hz (non-adjustable parameters of the device). Electrodes were fixed to the earlobe for sham stimulation or the cymba conchae for verum stimulation, respectively.

All study participants were instructed to stay awake, keep eyes open, and avoid movement for the total duration of the scan. To minimize artifacts due to electrical fields, the stimulation device was placed outside the scanner room and the wire entering the scanner room was shielded. Due to interferences with the Bluetooth connected pulse oximeter and breathing belt with the taVNS device, acquisition of typical physiological parameters was not possible. Both fMRI sessions were task-free and were separated by a 10 min break to minimize carry-over so-

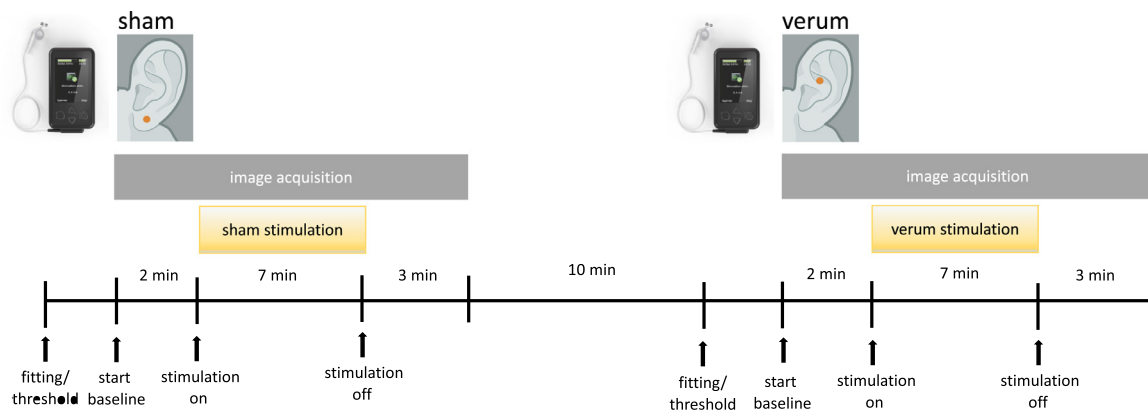


**Fig. 1.** Study design for testing sham-controlled transcutaneous auricular vagus nerve stimulation (taVNS) within the fMRI scanner. All volunteers received both, sham (left earlobe) and verum (left cymba conchae) stimulation on one testing day, with a break between the two fMRI sessions. To avoid carry-over effects, the first fMRI session was always acquired with a sham stimulation, and the subsequent with a verum stimulation. After entering the scanner, participants' individual sensory and pain thresholds were defined. Then, the fMRI started with a 2 min baseline (stimulation OFF), continued with a 7 min stimulation period (sham or verum), and ended with a 3 min post-stimulation period (stimulation OFF).

matosensory stimulation effects. Each session lasted 12 min, starting with a 2 min baseline phase, followed by 7 min stimulation, and a 3 min post-stimulation phase.

### 2.3. Imaging parameters

Imaging was performed on a 3T MRI system (Siemens Magnetom Prisma, Erlangen, Germany). Anatomical scans were acquired previously on a separate day with a 12 channel array head coil with 128 sagittal slices that covered the whole brain (MPRAGE, TR 2300ms, TE 2.32ms, field of view  $256 \times 256 \times 192\text{mm}^3$ , voxel size  $0.9 \times 0.9 \times 0.9\text{mm}^3$ , 213 sagittal slices). Functional imaging data were acquired using a task-free paradigm ("resting state"), lasting 12 min for each of the two sessions (verum and sham condition). Acquisition of functional images was performed with a 32-channel head coil (Siemens, Erlangen, Germany) in 34 axial slices with a T2\*-weighted echo-planar imaging sequence (slice thickness: 2 mm; in-plane resolution:  $2 \times 2\text{mm}^2$ ; no distance factor; ascending interleaved in-plane acquisition; TR = 2000ms, TE = 30ms, field of view  $192 \times 192 \times 60\text{mm}^3$ ; PAT factor = 2). In addition, we acquired two images with reversed phase encoding directions (anterior–posterior or posterior–anterior) for the purpose of estimating and correcting susceptibility-induced distortion (with an otherwise identical protocol as the main functional measurement).

### 2.4. Data preprocessing

Functional MRI Data sets were pre-processed using the FMRIB Software Library (FSL version 5.08, [www.fmrib.ox.ac.uk/fsl](http://www.fmrib.ox.ac.uk/fsl)) according to Smith et al. (2013). The first 3 images were discarded from the final data set to avoid equilibration effects. Non-brain tissue was removed using the automated brain extraction tool (Smith, 2002) and images were re-oriented in space (FSL FLIRT, Jenkinson, 2005). Susceptibility induced distortions were corrected with FSL TOPUP (Andersson and Sotiropoulos, 2016) and time series were realigned to correct for head movements (Jenkinson et al., 2002). Data were spatially smoothed using a Gaussian kernel with a 3mm FWHM and high-pass temporal filtering was applied (FWHM = 100s). Structured artefacts were then removed using independent component analysis followed by FSL's ICA-based X-noisefier (Griffanti et al., 2014; Salimi-Khorshidi et al., 2014). Then, functional data were co-registered to the subject's T1-weighted image and normalized to Montreal Neurological Institute (MNI) standard space for statistical analysis.

### 2.5. Statistical analysis

Statistical data analysis was carried out using statistical parametric mapping (SPM, version 12, r7219; Wellcome Department of Imaging Neuroscience, London) in MATLAB (version 2016b, The MathWorks). For the first-level analysis, we specified a voxel-wise general linear model (GLM) by generating 1 min time bins out of the total of 12 min image acquisition for both stimulation conditions (verum and sham). This operation resulted in 12 individual time bins (2 baseline, 7 stimulation, 3 post-stimulation) for each condition, resulting in 24 regressors in each GLM. The realignment parameters and their derivatives (in total 24 motion parameters, see Friston et al., 1996), a matrix indicating motion outlier volumes, as well as average time-series from white matter and ventricular cerebrospinal fluid were specified as nuisance regressors, to supplement the motion-based denoising with fMRI-signal-based denoising, see Power et al. (2015).

To assess individual stimulation effects over time, relative to the initial baseline activity, we subtracted the average BOLD response of the 2 min baseline from the average BOLD response of each and every stimulation and post-stimulation time bin (e.g., first verum time bin weighted with 1, and the two verum baseline time bins with -0.5 each, and so on). This was done separately for sham and verum regressors, respectively, meaning that each sham time bin was contrasted against the sham baseline, and each verum time bin against the verum baseline. As a result, ten contrast images for the sham condition and ten contrast images for the verum condition were computed.

In the second-level analysis, we specified a flexible factorial design with the factors subject and condition (10 sham and 10 verum contrasts from the 1<sup>st</sup> level) using a random-effects model. As we were particularly interested in brainstem responses, the second-level analysis was restricted to an anatomically-defined brainstem mask that excludes areas of high physiological noise (Beissner et al., 2014). We first compared all verum contrasts [contrast weights: ones(1,10)] against all sham contrasts [contrast weights:  $-1 \cdot \text{ones}(1,10)$ ], in order to identify brainstem regions that generally increase their activity in response to taVNS, spanning both the acute stimulation and the post-stimulation period. Next, we differentiated between the acute and late taVNS effects, by comparing verum versus sham selectively for the stimulation period and for the post-stimulation period, respectively. Significance threshold was set to  $p < 0.05$ , family-wise-error (FWE) corrected for multiple comparisons at the cluster level with a cluster-defining threshold of  $p < 0.001$ . Notably, under this cluster-defining threshold, cluster-level correction for multiple comparisons ensures a valid false positive rate control (Eklund et al., 2016; Flandin and Friston, 2019).

**Table 1**  
Brainstem regions with significant activation in response to taVNS.

	Region	Laterality	Cluster size	Cluster $p_{\text{fwe-corr}}$	x	y	z	T
<b>a) Verum &gt; sham: stimulation and post-stimulation</b>								
DRN	b	84	< 0.001	0	-30	-36	9.36	
SN	r	76	< 0.001	12	-14	-14	5.95	
STN	r			16	-16	6	6.13	
NTS	r	29	0.001	2	-40	-44	7.25	
SN	l	17	0.008	-12	-16	-12	6.82	
RN	r	44	< 0.001	4	-24	-12	6.44	
RN	l			-6	-22	-12	6.02	
GPI	r	17	0.008	12	0	-8	5.74	
NST	r	34	< 0.001	4	-46	-54	5.69	
<b>b) Verum &gt; sham: stimulation phase</b>								
DRN	b	20	0.004	0	-30	-36	6.67	
NTS	l	18	0.007	2	-38	-44	5.95	
SN	r	45	< 0.001	12	-14	-14	5.59	
RN	r	26	0.001	4	-24	-12	4.87	
IPN	b	13	0.024	4	-18	-28	4.87	
GPI	r	11	0.041	14	-4	-6	4.69	
STN	r			16	-16	6	5.16	
<b>c) Verum &gt; sham: post-stimulation phase</b>								
DRN	b	88	< 0.001	0	-30	-36	8.85	
SN	r	64	< 0.001	12	-14	-14	8.37	
STN	r			18	-14	-8	4.97	
SN	l	20	0.004	-12	-16	-8	6.12	
NTS	l	24	0.002	2	-40	-44	6.12	
GPI	r	14	0.018	12	0	-8	6.05	
RN	l	14	0.018	-6	-22	-12	5.61	
NST	r	17	0.008	4	-46	-54	5.10	

*Note.* DRN, Dorsal Raphe Nucleus; SN, Substantia Nigra; STN, Subthalamic Nucleus; NTS, Nucleus of the Solitary Tract; RN, Red Nucleus (putatively retrorubral field); GPI, internal Globus Pallidus; NST, Spinal Trigeminal Nucleus; IPN, Interpeduncular Nucleus.

### 3. Results

We examined time-dependent effects of taVNS on brainstem neuronal responses by comparing consecutive 1-min time bins of activity during the verum stimulation against the sham stimulation. To identify possible carry-over effects of the taVNS that persist after stimulation, we differentiated between acute BOLD responses during the stimulation (7 min in total) and delayed BOLD responses during the post-stimulation period (3 min in total). Notably, each of the 1 min time bins represent increased responses within this time window relative to the initial sham or verum baseline, respectively.

#### 3.1. Sustained effects of taVNS on the brainstem

To identify sustained, i.e., both acute and persistent, effects of taVNS on the brainstem activity, we compared the average neural responses to verum versus sham, spanning both the stimulation and post-stimulation periods. We found clusters of significant activation in the dorsal raphe nucleus (DRN), right substantia nigra (SN), left NTS, right subthalamic nucleus (STN) and the area of the red nucleus, putatively the retrorubral field (RN; see [Table 1](#) and [Figs. 2 and 3](#)). A closer look at the timeline of BOLD signal in these regions plotted in [Fig. 3](#) revealed the signal dynamics over time. Notably, the BOLD signal increased over time during verum compared to sham condition, with the notable exception of the SN.

#### 3.2. Differentiation of acute and delayed effects of taVNS on the brainstem

Next, we explored whether the same brainstem regions, that generally responded to taVNS, were indeed both significantly activated during acute stimulation and showed a significant delayed activation after the stimulation was terminated. First, we identified acute effects of taVNS on the brainstem activity, by comparing the average neural responses to verum versus sham, but spanning only the seven stimulation time bins. Next, we focused on the delayed effects, by again comparing verum ver-

sus sham, but this time spanning only the three post-stimulation time bins. Most of the brainstem regions generally activated by acute taVNS and thereafter were indeed robustly activated after the termination of the stimulation (see [Table 1](#) and [Fig. 3](#)). That is, these regions clearly showed a carry-over effect by being significantly activated both during acute taVNS and in the post-stimulation phase. Particularly, activity in the midbrain did not significantly increase during the acute stimulation phase alone, but increased significantly specifically during the post-stimulation, showing a delayed taVNS effect ([Table 1](#)). Interestingly, the right RN was significantly activated only during the acute taVNS, while the left RN showed the opposite pattern, being significantly activated only during the post-stimulation phase.

### 4. Discussion

Transcutaneous auricular VNS is a potential tool to modulate brain activity in a minimally invasive manner. We investigated the temporal dynamics of effects of taVNS effects on neural responses in the brainstem during fMRI in a cohort of healthy lean study participants. We demonstrate that taVNS of the cymba conchae relative to sham stimulation of the earlobe activates regions in the caudal brainstem that are consistent with location of the NTS, the primary relay station for vagal afferent signals, and its downstream targets. In this way, we could confirm earlier studies reporting NTS activation during taVNS applied to the cymba conchae ([Frangos et al., 2015](#); [Yakunina et al., 2017](#)). In addition, our findings indicate that taVNS can not only modulate the activity of NTS neurons but also its –mainly dopaminergic– downstream targets. Acute taVNS induced neuronal response in dopaminergic midbrain regions, which underscores links of the vagal gut-to-brain axis to neuronal reward pathways, evidenced by more direct chemo- and optogenetic manipulations in mouse models ([Han et al., 2018](#); [Tan et al., 2020](#)). Here, by using an analysis technique frequently applied for the evaluation of neural responses in (psycho-) pharmacological studies (so-called ph-fMRI, cf. [Wandschneider and Koeppe, 2016](#)), we demonstrate time-dependent fluctuations in BOLD signal during acute stimulation and after termina-

### a. Lower brainstem

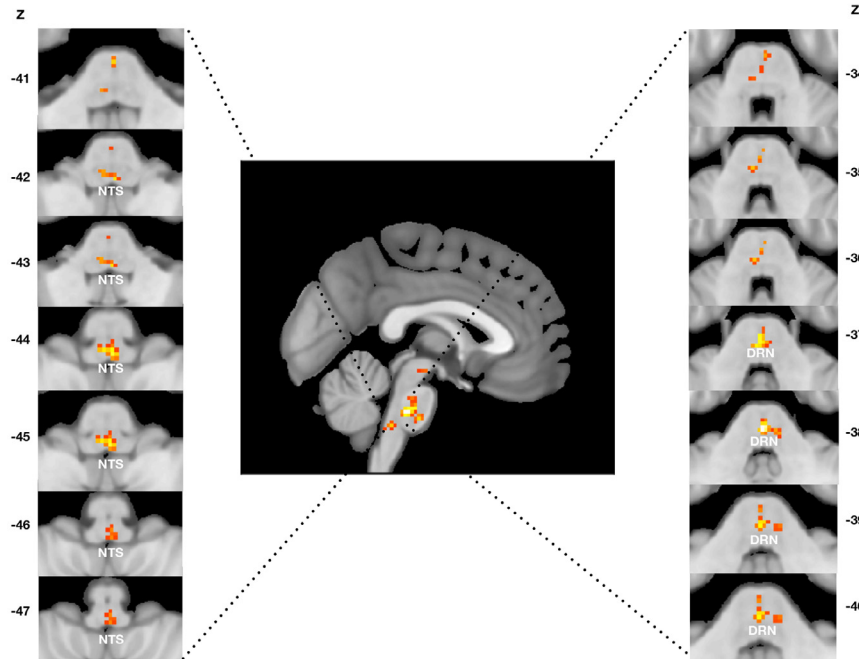
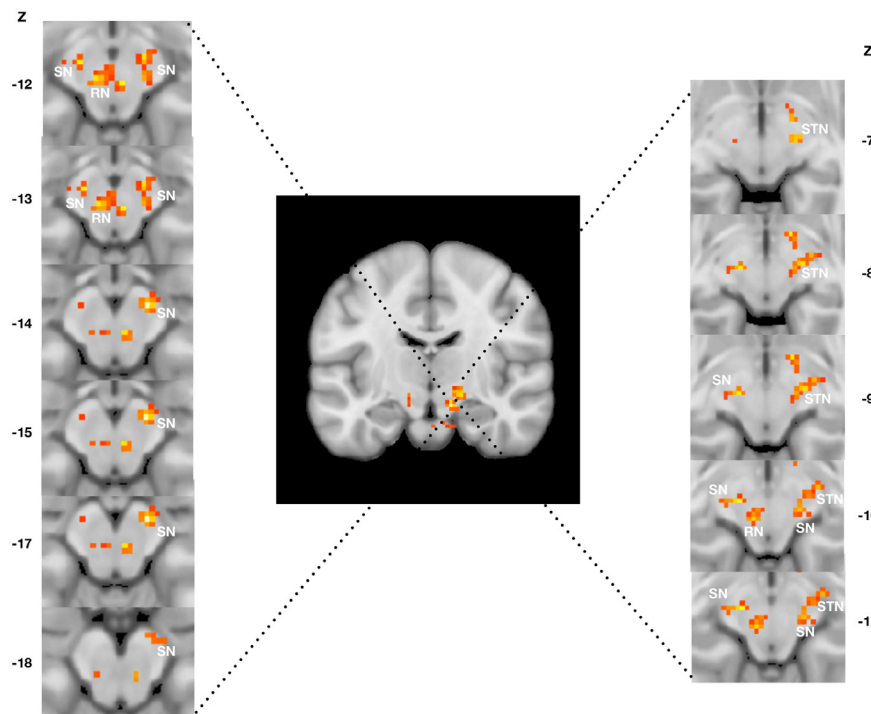


**Fig. 2.** Effects of taVNS on brainstem activity. Neural responses in the lower brainstem (a, medulla and pons) and the midbrain (b) were significantly increased during verum relative to sham stimulation. During both the acute stimulation and after the termination of the stimulation, the taVNS triggered BOLD responses in the nucleus of the solitary tract (NTS), the dorsal raphe nucleus (DRN), the substantia nigra (SN), the subthalamic nucleus (STN), and a region adjacent to the red nucleus (RN, putatively the retrorubral field). Significance threshold was set to  $p < 0.05$ , FWE-corrected for multiple comparisons at the cluster level within the brainstem mask, with a cluster-defining threshold of  $p < 0.001$ .

### b. Midbrain



tion which appear to be region-specific. With analysing time-dependent effect in BOLD signals, we are of course limited to the aperture of fMRI (Bright et al., 2017; Edwin Thanarajah et al., 2019; Tittgemeyer et al., 2018), and we can only measure a limited range of frequencies; this does not prevent us from finding an effect in the given range. To that end,

our study may provide the impetus for further studying the exact signal dynamic of the effect with different techniques.

Additionally, we note that our approach differs from conventional resting-state analysis of BOLD activation patterns, as average neuronal responses within consecutive 1-minute periods are expected to be dif-

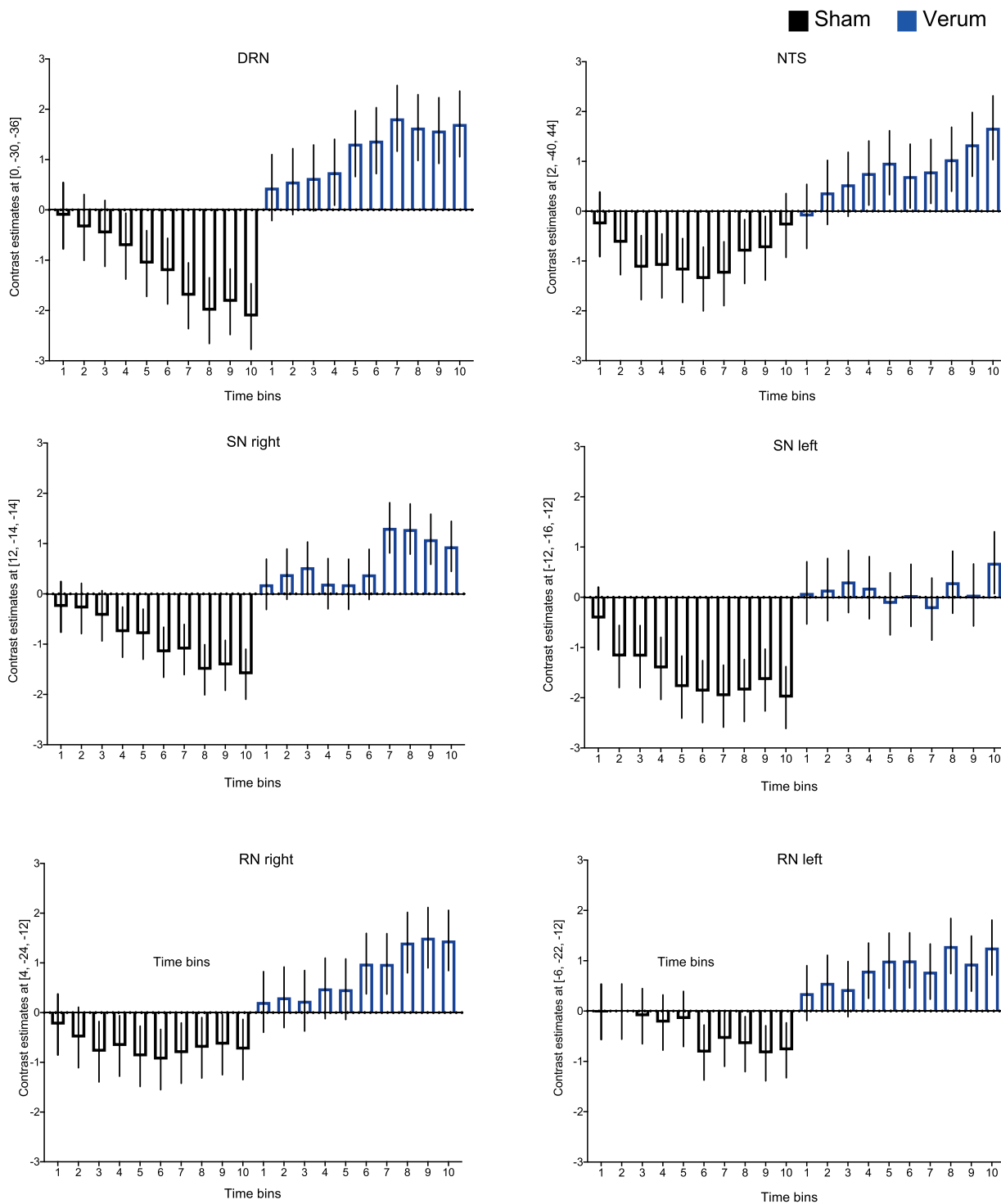


**Fig. 3.** Temporal dynamics of the effects of taVNS and sham stimulation on brainstem activity. We estimated the average BOLD response to consecutive 1-minute time bins, separately for verum and sham, each contrasted with the respective baseline (verum baseline or sham baseline). Both, verum and sham condition consisted of seven stimulation and three post-stimulation time bins. For the same brainstem regions revealing a significantly increased activity in response to taVNS relative to sham stimulation (cf Fig. 2), contrast estimates for the time bins are shown for the individual brainstem regions. Error bars show 90% CI. Note, the signal dynamics are highpass filtered such that slow dynamics on the time scale of ~2 min are filtered out.

ferentially modulated by taVNS relative to sham stimulation. The effect is outlined by some examples: While DRN activity increased, consistent with increased DRN firing rates in the rat following long term VNS (Manta et al., 2013), we could show a fluctuation of the NTS activity over the stimulation time, including prolonged increases in activity after the termination of the stimulation. This confirms our hypothesis of

carry-over effects of taVNS even after acute stimulation and their modulatory action on NTS activity.

However, given that the stimulation device likely also concurrently stimulated facial and trigeminal nerves, we cannot fully conclude activations to be exclusively vagally transmitted. This demands for stimulation devices with higher specificity, like for percutaneous VNS described pre-

viously (Kaniusas et al., 2019a). Still, our results are based on contrast estimates between the verum and the sham stimulation, which mitigates this confound as facial and trigeminal nerves are also stimulated in the sham condition, where the earlobe is targeted that is unlikely to be innervated by the vagus nerve (Butt et al., 2020). Together, these arguments are in favour of a rather specific stimulation of the vagal afferents.

Transcutaneous VNS has been shown to influence sympathetic outflow, leading to a shift towards parasympathetic control (Bretherton et al., 2019). Modulation of heart rate variability and cardiac output, in turn, presumably influence BOLD responses; hence, the lack of physiological recordings display a clear limitation of this study. We attempted to account for this drawback by performing an ICA in combination with FSL FIX with a moderately low filtering threshold to filter out physiological noise while compromising between the loss of signal and false positives – an approach which has been also followed in other fMRI studies aiming to decipher neural signatures of peripheral signals in the brainstem (e.g., Manuel et al., 2020; Power et al., 2015). In addition, we applied an anatomically-defined brainstem mask in order to exclude areas of high physiological noise (Beissner et al., 2014). By this means, we found activations in the caudal medulla, consistent with the location of the NTS, which fluctuated over the time course of stimulation, and thus conclude a (direct) pathway of the auricular branch of the vagus nerve to the NTS being activated by our stimulation protocol.

A crucial limitation of the currently available taVNS stimulation procedures is that effects on neurotransmitter and sympathetic activity have been shown, in animal studies, to be amplitude and frequency dependent (Noller et al., 2019). Although techniques to tune the stimulation more specifically towards physiological responses are available (Kaniusas et al., 2020), the analysis of underlying mechanisms in humans is restricted to stimulation parameters, which are mostly fixed for ready-to-use medical devices. Understanding the physiological correlates of taVNS demands for more explorative investigations of the effects of varying stimulation frequencies. However, this would require a tight control of cardiac function to avoid health compromising side effects like arrhythmias and bradycardia.

In sum, we provide an assessment of BOLD signal dynamics in response to taVNS with a commonly used stimulation device, which have set parameters for stimulation amplitude and frequency. We show that taVNS activates the primary afferent targets of the vagus nerve, the NTS, and (putatively dopaminergic) downstream regions within the brainstem. In future, studies focussing on fine-tuning the stimulation parameters to more specific physiological responses and extending their analysis to the whole brain are needed to further elaborate neuromodulatory effects of taVNS.

#### Data availability statement

All data will be made available upon request. The request necessitates that the purpose of data re-analysis is in line with the study aims as approved by the ethics review board (see text) and participants consent. Furthermore, consent to data privacy need to be assured by signing an agreement form accordingly.

#### Declaration of Competing Interest

The authors declare no competing financial interests. M.T. is supported by funding from the German Centre for Diabetes Research (DZD) – Project-ID 82DZD00502 & 82DZD03C2G as well as by the Deutsche Forschungsgemeinschaft (DFG, German Research Foundation) – Project-ID 431549029 – SFB 1451. H.F. and M.T. are also funded by the Deutsche Forschungsgemeinschaft (DFG, German Research Foundation) under Germany's Excellence Strategy – EXC 2030 – 390661388. H.F. received funding from the European Union through the ERC Starting Grant “GuMeCo”.

#### Credit authorship contribution statement

**Diba Borgmann:** Data curation, Formal analysis, Investigation, Project administration, Visualization, Writing – original draft. **Lionel Rigoux:** Formal analysis, Methodology, Software. **Bojana Kuzmanovic:** Formal analysis, Visualization. **Sharmili Edwin Thanarajah:** Conceptualization. **Thomas F. Münte:** Conceptualization, Funding acquisition. **Henning Fenselau:** Supervision, Writing – review & editing. **Marc Tittgemeyer:** Conceptualization, Supervision, Funding acquisition, Writing – original draft.

#### Acknowledgements

The authors wish to thank first of all Alberto Gonzáles Olmos for engaging in a prior project phase to test the taVNS stimulator under MR conditions. Furthermore, we are grateful for Patrick Weyer and Timm Wetzel for their outstanding support in data acquisition.

#### References

- Alhadeff, A.L., 2021. Monitoring in vivo neural activity to understand gut-brain signaling. *Endocrinology* 162, bqab029. doi:10.1210/endo/bqab029.
- Alicart, H., Heldmann, M., Gottlich, M., Obst, M.A., Tittgemeyer, M., Münte, T.F., 2020. Modulation of visual processing of food by transcutaneous vagus nerve stimulation (tVNS). *Brain Imaging Behav.* 1–12. doi:10.1007/s11682-020-00382-8.
- Andersson, J.L.R., Sotiropoulos, S.N., 2016. An integrated approach to correction for off-resonance effects and subject movement in diffusion MR imaging. *Neuroimage* 125, 1063–1078. doi:10.1016/j.neuroimage.2015.10.019.
- Aston-Jones, G., Zhu, Y., Card, J.P., 2004. Numerous GABAergic afferents to locus ceruleus in the pericellular dendritic zone: possible interneuronal pool. *J. Neurosci.* 24, 2313–2321. doi:10.1523/JNEUROSCI.5339-03.2004.
- Bai, L., Mesgarzadeh, S., Ramesh, K.S., Huey, E.L., Liu, Y., Gray, L.A., Aitken, T.J., Chen, Y., Beutler, L.R., Ahn, J.S., et al., 2019. Genetic identification of vagal sensory neurons that control feeding. *Cell* 179, 1129–1143. doi:10.1016/j.cell.2019.10.031, e1123.
- Barraco, I., 1994. *Nucleus of the Solitary Tract*. CRC Press.
- Beissner, F., Schumann, A., Brunn, F., Eisenträger, D., Bar, K.J., 2014. Advances in functional magnetic resonance imaging of the human brainstem. *Neuroimage* 86, 91–98. doi:10.1016/j.neuroimage.2013.07.081.
- Ben-Menachem, E., Hamberger, A., Hedner, T., Hammond, E.J., Uthman, B.M., Slater, J., Treig, T., Stefan, H., Ramsay, R.E., Wernicke, J.F., et al., 1995. Effects of vagus nerve stimulation on amino acids and other metabolites in the CSF of patients with partial seizures. *Epilepsy Res.* 20, 221–227. doi:10.1016/0920-1211(94)00083-9.
- Borgmann, D., Ciglieri, E., Biglari, N., Brandt, C., Cremer, A.L., Backes, H., Tittgemeyer, M., Wunderlich, F.T., Bruning, J.C., Fenselau, H., 2021. Gut-brain communication by distinct sensory neurons differently controls feeding and glucose metabolism. *Cell Metab.* 33, 1466–1482. doi:10.1016/j.cmet.2021.05.002, e1467.
- Bretherton, B., Atkinson, L., Murray, A., Clancy, J., Deuchars, S., Deuchars, J., 2019. Effects of transcutaneous vagus nerve stimulation in individuals aged 55 years or above: potential benefits of daily stimulation. *Aging (Albany NY)* 11, 4836–4857. doi:10.18632/aging.102074.
- Bright, M.G., Tench, C.R., Murphy, K., 2017. Potential pitfalls when denoising resting state fMRI data using nuisance regression. *Neuroimage* 154, 159–168. doi:10.1016/j.neuroimage.2016.12.027, PMID -28025128.
- Brown, R.E., Sergeeva, O.A., Eriksson, K.S., Haas, H.L., 2002. Convergent excitation of dorsal raphe serotonin neurons by multiple arousal systems (orexin/hypocretin, histamine and noradrenaline). *J. Neurosci.* 22, 8850–8859. doi:10.1523/jneurosci.22-20-08850.2002.
- Butt, M.F., Albusoda, A., Farmer, A.D., Aziz, Q., 2020. The anatomical basis for transcutaneous auricular vagus nerve stimulation. *J. Anat.* 236, 588–611. doi:10.1111/joa.13122.
- Ch'ng, S., Fu, J., Brown, R.M., McDougall, S.J., Lawrence, A.J., 2018. The intersection of stress and reward: BNST modulation of aversive and appetitive states. *Prog. Neuropsychopharmacol. Biol. Psychiatry* 87, 108–125. doi:10.1016/j.pnpbp.2018.01.005.
- Chen, J., Cheng, M., Wang, L., Zhang, L., Xu, D., Cao, P., Wang, F., Herzog, H., Song, S., Zhan, C., 2020. A vagal-NTS neural pathway that stimulates feeding. *Curr. Biol.* 30, 3986–3998. doi:10.1016/j.cub.2020.07.084, e3985.
- Clemmensen, C., Müller, T.D., Woods, S.C., Berthoud, H.R., Seeley, R.J., Tschöp, M.H., 2017. Gut-brain cross-talk in metabolic control. *Cell* 168, 758–774. doi:10.1016/j.cell.2017.01.025.
- Colzato, L., Beste, C., 2020. A literature review on the neurophysiological underpinnings and cognitive effects of transcutaneous vagus nerve stimulation: challenges and future directions. *J. Neurophysiol.* 123, 1739–1755. doi:10.1152/jn.00057.2020.
- Cork, S.C., 2018. The role of the vagus nerve in appetite control: Implications for the pathogenesis of obesity. *J. Neuroendocrinol.* 30, e12643. doi:10.1111/jne.12643.
- Cutsforth-Gregory, J.K., Benarroch, E.E., 2017. Nucleus of the solitary tract, medullary reflexes, and clinical implications. *Neurology* 88, 1187–1196. doi:10.1212/WNL.0000000000003751.
- de Lartigue, G., 2016. Role of the vagus nerve in the development and treatment of diet-induced obesity. *J. Physiol.* 594, 5791–5815. doi:10.1113/JP271538.

- Dorr, A.E., Debonnel, G., 2006. Effect of vagus nerve stimulation on serotonergic and noradrenergic transmission. *J. Pharmacol. Exp. Ther.* 318, 890–898. doi:10.1124/jpet.106.104166.
- Edwin Thanarajah, S., Iglesias, S., Kuzmanovic, B., Rigoux, L., Stephan, K.E., Bruning, J.C., Tittgemeyer, M., 2019. Modulation of midbrain neurocircuitry by intranasal insulin. *Neuroimage* 194, 120–127. doi:10.1016/j.neuroimage.2019.03.050.
- Egerod, K.L., Schwartz, T.W., Gautron, L., 2019. The molecular diversity of vagal afferents revealed. *Trends Neurosci.* 42, 663–666. doi:10.1016/j.tins.2019.08.002.
- Eklund, A., Nichols, T.E., Knutsson, H., 2016. Cluster failure: why fMRI inferences for spatial extent have inflated false-positive rates. *Proc. Natl. Acad. Sci. U. S. A.* 113, 7900–7905. doi:10.1073/pnas.1602413113.
- Fang, J., Rong, P., Hong, Y., Fan, Y., Liu, J., Wang, H., Zhang, G., Chen, X., Shi, S., Wang, L., et al., 2016. Transcutaneous vagus nerve stimulation modulates default mode network in major depressive disorder. *Biol. Psychiatry* 79, 266–273. doi:10.1016/j.biopsych.2015.03.025.
- Flandin, G., Friston, K.J., 2019. Analysis of family-wise error rates in statistical parametric mapping using random field theory. *Hum. Brain Mapp.* 40, 2052–2054. doi:10.1002/hbm.23839.
- Frangos, E., Ellrich, J., Komisaruk, B.R., 2015. Non-invasive access to the vagus nerve central projections via electrical stimulation of the external ear: fMRI evidence in humans. *Brain Stimul.* 8, 624–636. doi:10.1016/j.brs.2014.11.018.
- Friston, K.J., Williams, S., Howard, R., Frackowiak, R.S., Turner, R., 1996. Movement-related effects in fMRI time-series. *Magn. Reson. Med.* 35, 346–355. doi:10.1002/mrm.1910350312.
- Fülling, C., Dinan, T.G., Cryan, J.F., 2019. Gut microbe to brain signaling: what happens in vagus.... *Neuron* 101, 998–1002. doi:10.1016/j.neuron.2019.02.008, PMID -30897366.
- Goldstein, N., McKnight, A.D., Carty, J.R.E., Arnold, M., Betley, J.N., Alhadeff, A.L., 2021. Hypothalamic detection of macronutrients via multiple gut-brain pathways. *Cell Metab.* 33, 676–687. doi:10.1016/j.cmet.2020.12.018, e675.
- Griffanti, L., Salimi-Khorshidi, G., Beckmann, C.F., Auerbach, E.J., Douaud, G., Sexton, C.E., Zsoldos, E., Ebmeier, K.P., Filippini, N., Mackay, C.E., et al., 2014. ICA-based artefact removal and accelerated fMRI acquisition for improved resting state network imaging. *Neuroimage* 95, 232–247. doi:10.1016/j.neuroimage.2014.03.034.
- Hachem, L.D., Wong, S.M., Ibrahim, G.M., 2018. The vagus afferent network: emerging role in translational connectomics. *Neurosurg. Focus* 45, E2. doi:10.3171/2018.6.FOCUS18216.
- Han, W., Tellez, L.A., Perkins, M.H., Perez, I.O., Qu, T., Ferreira, J., Ferreira, T.L., Quinn, D., Liu, Z.W., Gao, X.B., et al., 2018. A Neural Circuit for Gut-Induced Reward. *Cell* 175, 665–678. doi:10.1016/j.cell.2018.08.049, e623.
- Jenkinson, M., 2005. BET2: MR-based estimation of brain, skull and scalp surfaces. *Eleventh Annual Meeting of the Organization for Human Brain Mapping*.
- Jenkinson, M., Bannister, P., Brady, M., Smith, S., 2002. Improved optimization for the robust and accurate linear registration and motion correction of brain images. *Neuroimage* 17, 825–841. doi:10.1016/s1053-8119(02)91132-8.
- Kaniusas, E., Kampusch, S., Tittgemeyer, M., Panetos, F., Gines, R.F., Papa, M., Kiss, A., Podesser, B., Cassara, A.M., Tanghe, E., et al., 2019a. Current directions in the auricular vagus nerve stimulation ii - an engineering perspective. *Front Neurosci.* 13, 772. doi:10.3389/fnins.2019.00772.
- Kaniusas, E., Kampusch, S., Tittgemeyer, M., Panetos, F., Gines, R.F., Papa, M., Kiss, A., Podesser, B., Cassara, A.M., Tanghe, E., et al., 2019b. Current directions in the auricular vagus nerve stimulation I - a physiological perspective. *Front Neurosci.* 13, 854. doi:10.3389/fnins.2019.00854.
- Kaniusas, E., Samoudi, A.M., Kampusch, S., Bald, K., Tanghe, E., Martens, L., Joseph, W., Szeles, J.C., 2020. Stimulation pattern efficiency in percutaneous auricular vagus nerve stimulation: experimental versus numerical data. *IEEE Trans. Biomed. Eng.* 67, 1921–1935. doi:10.1109/TBME.2019.2950777.
- Keute, M., Demirezen, M., Graf, A., Mueller, N.G., Zaehle, T., 2019. No modulation of pupil size and event-related pupil response by transcutaneous auricular vagus nerve stimulation (taVNS). *Sci. Rep.* 9, 11452. doi:10.1038/s41598-019-47961-4.
- Keute, M., Ruhnau, P., Heinze, H.J., Zaehle, T., 2018. Behavioral and electrophysiological evidence for GABAergic modulation through transcutaneous vagus nerve stimulation. *Clin. Neurophysiol.* 129, 1789–1795. doi:10.1016/j.clinph.2018.05.026.
- Kim, K.-S., Seeley, R.J., Sandoval, D.A., 2018. Signalling from the periphery to the brain that regulates energy homeostasis. *Nat. Rev. Neurosci.* 19, 185–196. doi:10.1038/nrn.2018.8, PMID -29467468.
- Koenig, J., Parzer, P., Haigis, N., Liebmann, J., Jung, T., Resch, F., Kaess, M., 2021. Effects of acute transcutaneous vagus nerve stimulation on emotion recognition in adolescent depression. *Psychol. Med.* 51, 511–520. doi:10.1017/S0033291719003490.
- Kraus, T., Kiess, O., Hosl, K., Terekhin, P., Kornhuber, J., Forster, C., 2013. CNS BOLD fMRI effects of sham-controlled transcutaneous electrical nerve stimulation in the left outer auditory canal - a pilot study. *Brain Stimul.* 6, 798–804. doi:10.1016/j.brs.2013.01.011.
- Kühnel, A., Teckentrup, V., Neuser, M.P., Huys, Q.J.M., Burrasch, C., Walter, M., Kroemer, N.B., 2020. Stimulation of the vagus nerve reduces learning in a go/no-go reinforcement learning task. *Eur. Neuropsychopharmacol.* 35, 17–29. doi:10.1016/j.euroneuro.2020.03.023.
- Lebow, M.A., Chen, A., 2016. Overshadowed by the amygdala: the bed nucleus of the stria terminalis emerges as key to psychiatric disorders. *Mol Psychiatry* 21, 450–463. doi:10.1038/mp.2016.1, PMID -26878891.
- Liu, C.H., Yang, M.H., Zhang, G.Z., Wang, X.X., Li, B., Li, M., Woelfer, M., Walter, M., Wang, L., 2020. Neural networks and the anti-inflammatory effect of transcutaneous auricular vagus nerve stimulation in depression. *J. Neuroinflammation* 17, 54. doi:10.1186/s12974-020-01732-5.
- Manta, S., El Mansari, M., Debonnel, G., Blier, P., 2013. Electrophysiological and neurochemical effects of long-term vagus nerve stimulation on the rat monoaminergic systems. *Int. J. Neuropsychopharmacol.* 16, 459–470. doi:10.1017/S1461145712000387.
- Manuel, J., Farber, N., Gerlach, D.A., Heusser, K., Jordan, J., Tank, J., Beissner, F., 2020. Deciphering the neural signature of human cardiovascular regulation. *Elife* 9, e55316. doi:10.7554/eLife.55316.
- Neuser, M.P., Teckentrup, V., Kühnel, A., Hallschmid, M., Walter, M., Kroemer, N.B., 2020. Vagus nerve stimulation boosts the drive to work for rewards. *Nat. Commun.* 11, 3555. doi:10.1038/s41467-020-17344-9.
- Noller, C.M., Levine, Y.A., Urakov, T.M., Aronson, J.P., Nash, M.S., 2019. Vagus nerve stimulation in rodent models: an overview of technical considerations. *Front Neurosci* 13, 911. doi:10.3389/fnins.2019.00911.
- Obst, M.A., Heldmann, M., Alicart, H., Tittgemeyer, M., Munte, T.F., 2020. Effect of short-term transcutaneous vagus nerve stimulation (tVNS) on brain processing of food cues: an electrophysiological study. *Front. Hum. Neurosci.* 14, 206. doi:10.3389/fnhum.2020.00206.
- Power, J.D., Schlaggar, B.L., Petersen, S.E., 2015. Recent progress and outstanding issues in motion correction in resting state fMRI. *Neuroimage* 105, 536–551. doi:10.1016/j.neuroimage.2014.10.044.
- Salimi-Khorshidi, G., Douaud, G., Beckmann, C.F., Glasser, M.F., Griffanti, L., Smith, S.M., 2014. Automatic denoising of functional MRI data: combining independent component analysis and hierarchical fusion of classifiers. *Neuroimage* 90, 449–468. doi:10.1016/j.neuroimage.2013.11.046.
- Smith, S.M., 2002. Fast robust automated brain extraction. *Hum. Brain Mapp.* 17, 143–155. doi:10.1002/hbm.10062.
- Smith, S.M., Beckmann, C.F., Andersson, J., Auerbach, E.J., Bijsterbosch, J., Douaud, G., Duff, E., Feinberg, D.A., Griffanti, L., Harms, M.P., et al., 2013. Resting-state fMRI in the human connectome project. *Neuroimage* 80, 144–168. doi:10.1016/j.neuroimage.2013.05.039.
- Stamatakis, A.M., Sparta, D.R., Jennings, J.H., McElligott, Z.A., Decot, H., Stuber, G.D., 2014. Amygdala and bed nucleus of the stria terminalis circuitry: Implications for addiction-related behaviors. *Neuropharmacology* 76 Pt B, 320–328. doi:10.1016/j.neuropharm.2013.05.046.
- Szeska, C., Richter, J., Wendt, J., Weymar, M., Hamm, A.O., 2020. Promoting long-term inhibition of human fear responses by non-invasive transcutaneous vagus nerve stimulation during extinction training. *Sci. Rep.* 10, 1529. doi:10.1038/s41598-020-58412-w.
- Tan, H.E., Sisti, A.C., Jin, H., Vignovich, M., Villavicencio, M., Tsang, K.S., Goffer, Y., Zuker, C.S., 2020. The gut-brain axis mediates sugar preference. *Nature* 580, 511–516. doi:10.1038/s41586-020-2199-7.
- Tittgemeyer, M., Rigoux, L., Knösche, T.R., 2018. Cortical parcellation based on structural connectivity: A case for generative models. *Neuroimage* 173, 592–603. doi:10.1016/j.neuroimage.2018.01.077, PMID -29407457.
- Travagli, R.A., Anselmi, L., 2016. Vagal neurocircuitry and its influence on gastric motility. *Nat. Rev. Gastroenterol. Hepatol.* 13, 389–401. doi:10.1038/nrgastro.2016.76.
- von Wrede, R., Rings, T., Schach, S., Helmstaedter, C., Lehnertz, K., 2021. Transcutaneous auricular vagus nerve stimulation induces stabilizing modifications in large-scale functional brain networks: towards understanding the effects of taVNS in subjects with epilepsy. *Sci. Rep.* 11, 7906. doi:10.1038/s41598-021-87032-1, PMID -33846432.
- Wandschneider, B., Koeppe, M.J., 2016. PharmacofMRI: Determining the functional anatomy of the effects of medication. *Neuroimage Clin* 12, 691–697. doi:10.1016/j.nicl.2016.10.002.
- Warren, C.M., Tona, K.D., Ouwwerkerk, L., van Paridon, J., Poletiek, F., van Steenberg, H., Bosch, J.A., Nieuwenhuis, S., 2019. The neuromodulatory and hormonal effects of transcutaneous vagus nerve stimulation as evidenced by salivary alpha amylase, salivary cortisol, pupil diameter, and the P3 event-related potential. *Brain Stimul.* 12, 635–642. doi:10.1016/j.brs.2018.12.224.
- Yakunina, N., Kim, S.S., Nam, E.C., 2017. Optimization of transcutaneous vagus nerve stimulation using functional MRI. *Neuromodulation* 20, 290–300. doi:10.1111/ner.12541.
- Yu, C.D., Xu, Q.J., Chang, R.B., 2020. Vagal sensory neurons and gut-brain signaling. *Curr. Opin. Neurobiol.* 62, 133–140. doi:10.1016/j.conb.2020.03.006.